

## Demonstration of Robust Micromachined Jet Technology and Its Application to Realistic Flow Control Problems

Sung Pil Chang\*

*Department of Electronic and Electrical Engineering, Inha University,  
253 Younghyun3-Dong, Nam-Gu, Incheon 402-751, Korea*

This paper describes the demonstration of successful fabrication and initial characterization of micromachined pressure sensors and micromachined jets (microjets) fabricated for use in macro flow control and other applications. In this work, the microfabrication technology was investigated to create a micromachined fluidic control system with a goal of application in practical fluids problems, such as UAV (Unmanned Aerial Vehicle)-scale aerodynamic control. Approaches of this work include: (1) the development of suitable micromachined synthetic jets (microjets) as actuators, which obviate the need to physically extend micromachined structures into an external flow; and (2) a non-silicon alternative micromachining fabrication technology based on metallic substrates and lamination (in addition to traditional MEMS technologies) which will allow the realization of larger scale, more robust structures and larger array active areas for fluidic systems. As an initial study, an array of MEMS pressure sensors and an array of MEMS modulators for orifice-based control of microjets have been fabricated, and characterized. Both pressure sensors and modulators have been built using stainless steel as a substrate and a combination of lamination and traditional micromachining processes as fabrication technologies.

**Key Words :** MEMS, Micro Jet, Micro Fabrication, Capacitive Pressure Sensor, Lamination

### 1. Introduction

Micromachining is traditionally defined as the use of microfabrication technologies to create mechanical structures, potentially in addition to electronic devices, and MEMS are sensors and actuators (or systems containing sensors and actuators) fabricated using micromachining. The use of micromachining gives to MEMS the same advantages which integrated circuits enjoy, namely batch fabrication, and ease of realization and interconnection of large, cooperative actuators arrays. However, many MEMS actuators are small,

and this small size makes it difficult to generate sufficient force to influence macro-world events. There have been a number of efforts to use micro-actuators in fluids applications in spite of this small force generation, such as force-rebalanced microvalves and actuators placed at points of potential flow instabilities (Lang, 1999; Glezer and Amitay, 2002; Mallinson et al., 2001; Li and Ming, 2000; Lockerby and Carpenter, 2004). However, it would also be desirable in some applications to fabricate larger, more robust actuators capable of generating larger forces per actuator. In addition, it is often desirable to cover a 'large' (in the macro sense) area of a structure with actuators in order to influence the behavior of the entire structure.

Usually, micromachined devices have been realized using silicon substrates (Baltes, 1997; MacDonald, 1996; Howe, 1994; Mastrangelo et al., 1995). In many applications, the use of tradition-

---

\* Corresponding Author.

**E-mail :** spchang@inha.ac.kr

**TEL :** +82-32-860-7422; **FAX :** +82-32-868-3654

Department of Electronic and Electrical Engineering, Inha University, 253 Younghyun3-Dong, Nam-Gu, Incheon 402-751, Korea. (Manuscript **Received** August 26, 2005; **Revised** February 16, 2005)

al silicon-substrate micromachined devices may be limited, for example by the lack of ability of the surrounding silicon substrate to absorb large mechanical shocks. In this work, the use of more robust substrates have been investigated as suitable starting points for both bulk and surface micromachined structures, as well as investigated the possibility of the substrate forming essential structural components of the device package. Alternative fabrication techniques, such as techniques more commonly used in either conventional micromachining as well as electronic packaging microfabrication (e.g., lamination), are combined with traditional integrated-circuit-based microelectronics processing techniques to create micromachined devices on these robust substrates.

One of the advantages of the use of robust substrates is the possibility of co-fabrication of the micromachined devices and their packages using, e.g., the robust substrate itself as an integral part of the sensor or actuator package. Another advantage is that due to substrate robustness, these co-packaged devices may be able to be used in mechanically harsh environments, such as aerodynamic applications. Finally, it is envisioned that the larger-scale devices (especially actuators) producible by this fabrication technology will have increased control authority over their silicon counterparts.

The use of synthetic jets (James et al., 1996) as fluidic actuators enables the possibility of altering the apparent aerodynamic shape of an airfoil by creating a closed recirculation region without extending any mechanical parts into the cross flow of the airfoil. This approach is very suitable for a MEMS-based flow control scheme, since (1) such devices have already been demonstrated as being compatible with micromachining technology (Coe et al., 1994); and (2) the relatively 'delicate' MEMS devices do not need to be exposed to the flow; in fact, the devices can be recessed under an orifice plate, safely out of reach of the flow. A microjet, pressure sensor, and provision for integrated circuitry can also be combined together to form a module suitable for repetition into an array. Such a module contains a modulator to switch the synthetic jets on and

off at each orifice hole, a pressure sensor to sense the local pressure, and some local electronics to perform readout, signal linearization, and/or local control.

## 2. Micromachined Capacitive Pressure Sensor

A robust capacitive pressure sensor array has been fabricated using stainless steel as a substrate, stainless steel film as a pressure-sensitive flexible plate, and electroplated nickel as a back electrode. By sensing the capacitance change of the capacitor formed between the flexible diaphragm and the rigid backplate (Fig. 1), and by knowing the mechanical properties of the diaphragm, the pressure can be determined.

An important attribute of this design is that only the steel substrate and the pressure sensor inlet is exposed to the flow; i.e., the sensor is self-packaged.

The sensor device concept is based on the pressure-induced deflection of a metallized flexible plate and the subsequent measurement of the capacitance between this deflecting plate and a fixed surface micromachined backplate positioned over the plate. Figure 1 shows a schematic diagram of the side-view of the device, where  $t_g$  is an initial gap distance between the fixed electrode and the flexible plate electrode,  $w_o$  is the deflection at the center of the plate,  $t_m$  is the thickness of the plate,

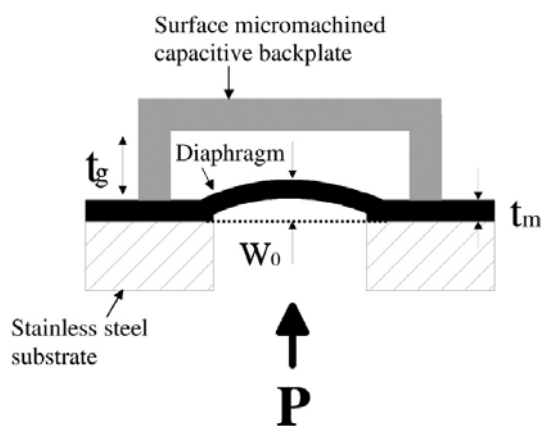


Fig. 1 A schematic diagram of the side-view of the capacitive pressure sensor

and  $P$  is the uniform applied pressure. For analytical modeling (Timoshenko, 1940), several assumptions have been made: (1) neglect stretching of the plate; (2) neglect the thickness of the metallic electrode on the plate; (3) neglect residual stress in the plate; and (4) neglect electric field fringing effects. Under these conditions, the capacitance–pressure relationship of the sensor can be shown to be:

$$C_{\text{sensor}} = C_0(1 + K_1P + K_2P^2 + \dots) \quad (1)$$

where  $K_n$  are constants given by:

$$K_n = \frac{1}{(2n+1)} \left[ \frac{a^4}{64Dt_g} \right]^n \quad (2)$$

for  $n \geq 1$ ,  $C_0$  is the undeflected capacitance,  $a$  is the radius of the diaphragm, and  $D$  is the flexural rigidity of the diaphragm.

The fabrication sequence of stainless steel diaphragm pressure sensors is shown in Fig. 2. The process starts on square, stainless steel substrates that are each 6.0 cm on a side, 0.8 mm thick, and have surface roughness of approximately 6–8  $\mu\text{m}$ . A  $6 \times 6$  array of pressure inlet holes with a diameter of 2 mm, with 7 mm center-to-center distances, is milled through the stainless steel substrates. A stainless steel sheet (Precision Brand Product, INC) is laminated onto the milled stainless steel substrate using a hot press with a pressure of 8.65 MPa and a temperature of 175°C for 30 min.

The stainless steel sheet is used as the pressure

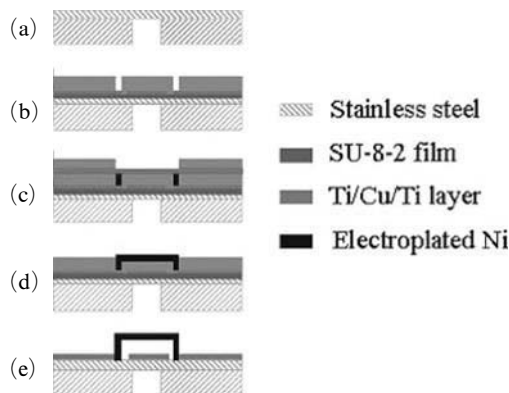


**Fig. 2** Fabrication sequence of pressure sensor based on stainless steel diaphragm

sensitive diaphragm and has a thickness of 12.7  $\mu\text{m}$  and surface roughness of approximately 100Å. Reactive ion etching (RIE) is then used to remove any exposed epoxy resin under the stainless steel diaphragm that has leaked through the pressure inlet holes (Fig. 2(a)).

A 250 Å thick titanium layer is deposited as an adhesion layer, and a 7  $\mu\text{m}$  thick epoxy resist SU-8-2 (MicroChem Corp.) is deposited as an insulation layer. To create bottom electrodes, electroplating seed layers, and bonding pads, Ti/Cu/Ti layers are deposited with a thickness of 250/6000/250 Å and patterned. AZ4620 photoresist (Clariant Corp.) is spun onto the patterned layer, yielding a final thickness of photoresist of approximately 25–27  $\mu\text{m}$  (Fig. 2(b)). The photoresist is patterned to create electroplating molds and nickel supports are electroplated through the molds.

To fabricate the backplate, a seed layer of Ti/Cu/Ti is deposited. Thick photoresist (AZ 4620) is spun on the seed layer (approximately ~25  $\mu\text{m}$  thick) and patterned to form electroplating molds. These molds are then filled with nickel by electroplating (Fig. 2(c)). And another seed layer and mold layer are coated and electroplated with nickel to form back plate (Fig. 2(d)). Finally, the photoresist sacrificial layers and the seed layers between them are etched to release the gap between the fixed backplate and the pressure sensitive stainless steel diaphragm (Fig. 2(e)). Figure 3 shows a photomicrograph of the fabricated stainless steel sensor array.

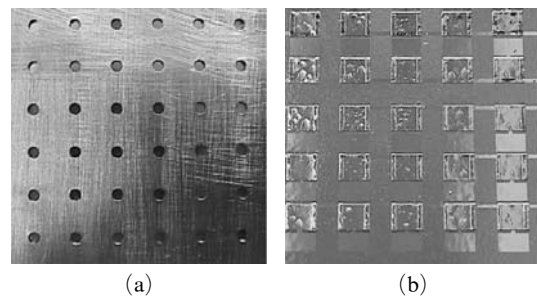


**Fig. 3** Photomicrographs of fabricated pressure sensors. (a) side exposed to environment. (b) rear view showing surface micromachined backplate

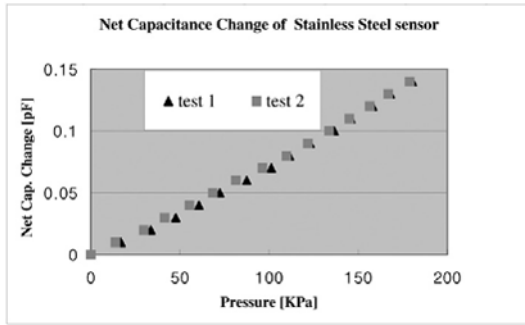


**Fig. 4** Net capacitance change versus pressure for capacitive pressure sensors

In order to characterize the capacitance of individual pressure sensors, measurements were carried out with a Keithley 3322 LCZ meter. The sensor device to be tested was mounted and sealed on a test fixture. The fixture was connected to a commercial pressure sensor (Fluke Corp. PV 350 Digital Pressure/Vacuum Module) and a digital multimeter to monitor the differential pressure. A compressed nitrogen line was connected to the fixture to serve as the pressure source with a regulator between them to control the differential pressure that would be applied to the fabricated devices. The LCZ meter was then connected to the fabricated sensors to obtain the characterization data for the capacitive pressure sensor. Capacitance versus pressure data of the stainless steel diaphragm based capacitive pressure sensor is shown in Fig. 4. For a range of applied pressure from 0 to 178 kPa, the net capacitance change was 0.14 pF. The sensitivities of the sensors were approximately 9.03 ppm/Kpa.

In order to reduce parasitic effects, a commercially available MS3110 Universal Capacitive Readout IC was used to obtain data in its un-packaged, die-form from Microsensors, Inc. This chip in its die-form was then integrated via wire-bonding to the microfabricated sensors. The MS 3110 senses the difference between two capacitors and outputs a voltage proportional to the difference. The output voltage can be described by a function of the sensing capacitances  $CS_{1T}$  and  $CS_{2T}$ , as shown by the following expression :

$$V_o = Gain * V_{2P25} * 1.14 * \frac{(CS_{2T} - CS_{1T})}{CF} + V_{ref} \quad (3)$$

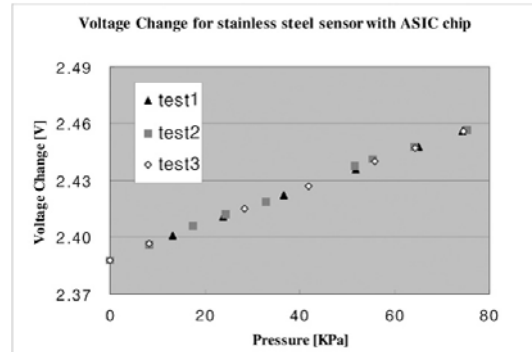


**Fig. 5** The voltage output of the MS3110 IC for the capacitive pressure sensor

Where  $CS_{2T}$  is the input from the microsensor being tested and  $CS_{1T}$  is the reference value as input from the reference microsensor. The gain is normally 2 V/V and V2P25 is the ASIC internal 2.25V DC reference, and CF is the capacitor feedback around the input trans-impedance amplifier, can be selected to optimize for the range of the input sensing capacitors.  $V_{ref}$  is 2.25 V.

Figure 5 shows the voltage output of the MS 3110 for the stainless-steel diaphragm sensor as a function of applied pressure from 0 to 75 kPa. The measured value of relative voltage change is 2.85% over the applied pressure range from 0 to 75 kPa. This sensor contained a gap of 21  $\mu\text{m}$  and a sensitivity of 0.92 mV/kPa.

### 3. Micromachined Microjet Modulator

A robust microjet modulator array has been fabricated using stainless steel as a substrate, Kapton film as an insulator, and thin stainless steel foil (12.7  $\mu\text{m}$  thick) as the modulator material. Microjet drivers have been assembled with these robust modulators and the velocity profiles of the MEMS-modulated synthetic jets for multiple numbers of modulators in an array has been measured using particle image velocimetry (PIV). The modulators operate by electrostatically opening and closing a plate which bears an array of holes and which covers the orifice plate. When the plate is in contact with the substrate, the substrate orifice hole is blocked and the synthetic jet cannot

issue from the orifice. When the plate is not in contact with the substrate, the synthetic jet can flow through the holes in the orifice plate and through the orifice hole in the substrate, thereby allowing a synthetic jet to issue from the orifice hole.

The fabrication sequence of the robust modulator array is shown in Fig. 6. The process starts on square 5.7 cm (2 inch) on a side, 0.5 mm thick stainless steel substrates. An array of  $5 \times 5$  orifice holes with a diameter of 2 mm, with 10 mm center-to-center distances, are milled through the substrate. Kapton film (Dupont, Kapton HN200, 50  $\mu\text{m}$  thick) is laminated onto the milled stainless steel using a hot press. Stainless steel foil (12.7  $\mu\text{m}$  thick : AISI-T302) is laminated again on top of the Kapton polyimide film using a hot press (Figure 6(a)).

Photoresist SC1813 (Shipley) is spun onto the laminated stainless steel foil. Photoresists are photo-defined and the stainless steel metal foil is wet etched by the mixture of HCl, H<sub>2</sub>O and FeCl<sub>3</sub> 6H<sub>2</sub>O. The modulation actuators will thus be formed by the stainless steel foil in the regions suspended over the milled orifice holes (Fig. 6(b)). Both of the Kapton film under the stainless steel foil and photoresist mask material have been isotropically dry etched using a barrel plasma etcher (Fig. 6(c) and 6(d)). Finally, a 5.6  $\mu\text{m}$  thick parylene film is conformally deposited for electrical insulation. Figure 7 shows the top view of the stainless steel modulator after the wet etching and the etched profile of Kapton polyimide film after isotropic dry etch.

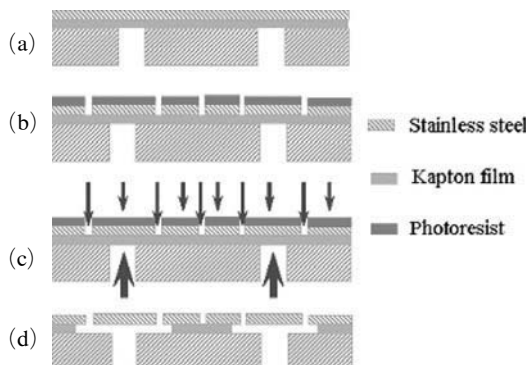


Fig. 6 Modulator fabrication sequence

After the fabrication of an array of robust modulator, the modulator array has been assembled with microjet drivers (Fig. 8). Both electromagnetic and piezoelectric drivers have been assembled and tested. The assembled robust modulator/jet driver has been tested using particle image velocimetry (PIV). Figure 9 shows raster plots of the velocity magnitude for three modulators with different diameter vent holes (the vent holes of the modulator at 10 mm [ $x$ -axis] is the largest and the one at 30 mm is the smallest) with all modulators open. This PIV test result shows that the robust modulator/jet driver can create jets with centerline speeds at  $y/d \approx 10$  (where  $d$  is the diameter of the orifice hole) of as

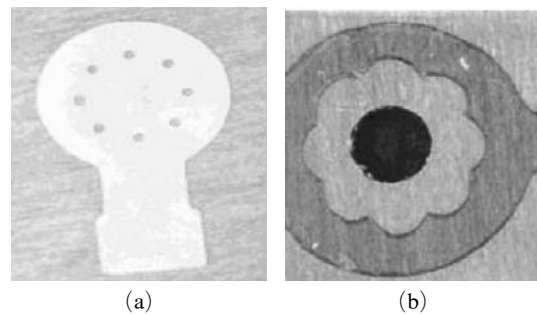


Fig. 7 (a) Top view of the stainless steel modulator after the wet etching. (b) Top view of the etched profile of Kapton polyimide film after isotropic dry etch

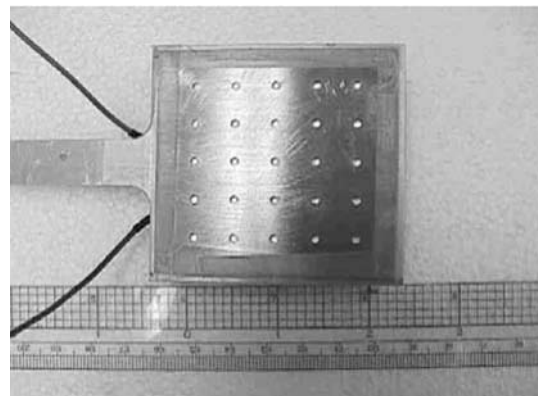
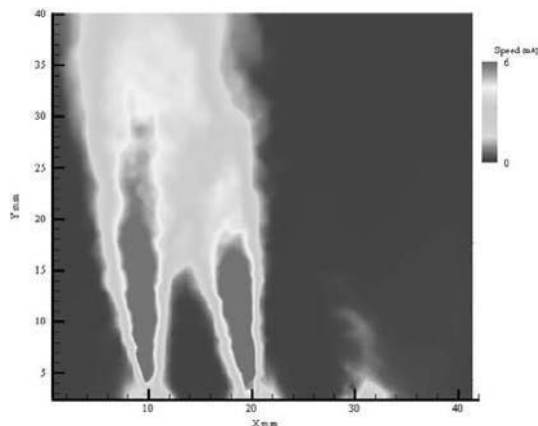


Fig. 8 An array of robust modulators assembled with a central microjet driver, showing the array of orifice holes. This view is what the external crossflow 'sees'



**Fig. 9** Velocity profile (PIV data) for the robust modulator array (three modulators with different diameters of vent holes shown)

much as 6 m/s.

#### 4. Conclusions

Stainless steel has been studied as a robust substrate and diaphragm material for micromachined devices. Lamination combined with traditional micromachining processes has been investigated as suitable fabrication methods for this robust substrate.

Capacitive pressure sensor has been designed, fabricated, and characterized by using lamination processing with stainless steel films as diaphragm on the stainless steel shim stock substrate. This sensor has a sensitivity of 9.03 ppm/Kpa with a net capacitance change of 0.14 pF over a range of 0 to 178 kPa.

To avoid the parasitic capacitance, the MS3110 IC in its un-packaged, die-type was integrated via wirebonding to the microfabricated sensors. The measured value of relative voltage change was 2.85% over the applied pressure range from 0 to 75 kPa. This sensor contained a gap of 21  $\mu\text{m}$  and had a sensitivity of 0.92 mV/Kpa

A robust modulator array using a robust stainless steel shim stock, Kapton film as an insulator, stainless steel metal foil as a modulator body has been designed, fabricated, and characterized. The PIV test for parts of robust modulator arrays show that microjets as high as 6 m/s can be

created using this device.

#### Acknowledgments

This work was supported by INHA UNIVERSITY Research Grant. (INHA-32735)

#### References

- Baltes, H., 1997, "CMOS Micro Electro Mechanical Systems," *Sensors and Materials*, Vol. 9, No. 6, pp. 331~346.
- Coe, D. J., Allen, M. G., Trautman, M. A. and Glezer, A., 1994, "Micromachined Jets for Manipulation of Macro Flows," in *Proceedings 1994 Solid-State Sensors and Actuators Workshop*, Hilton Head, SC, pp. 243~247.
- Glezer, A. and Amitay, M., 2002, "Synthetic Jets," *Annu. Rev. Fluid Mech.*, Vol. 34, pp. 503~529.
- Howe, R. T., 1994, "Applications of Silicon Micromachining to Resonator Fabrication," in *Proceedings of the 1994 IEEE International Frequency Control Symposium (The 48th Annual Symposium) (Cat. No.94CH3446-2)*, pp. 2~7.
- James, R. D., Jacob, J. W. and Glezer, A., 1996, "A Round Turbulent Jet Produced by an Oscillating Diaphragm," *Journal of Physics of Fluids*, Vol. 8, No. 9, pp. 2482~2495.
- Lang, W., 1999, "Reflections on the Future of Microsystems," *Sensors and Actuators*, Vol. 72, pp. 1~15.
- Li, Y. and Ming, X., 2000, "Control of Two-Dimensional Jets Using Miniature Zero Mass Flux Jets," *Chinese Journal of Aeronautics*, Vol. 13, No. 3, pp. 129~133.
- Lockerby, D. A. and Carpenter, P. W., 2004, "Modeling and Design of Micro-Jet Actuators," *AIAA J.*, Vol. 42, No. 2, pp. 220~227.
- MacDonald, N. C., 1996, "SCREAM Micro-electromechanical Systems," *Microelectronics Engineering*, Vol. 32, No. 1-4, pp. 49~73.
- Mallinson, S. G., Reizes, J. A. and Hong, G., 2001, "An Experimental and Numerical Study of Synthetic Jet Flow," *Aeronautical Journal*, Vol. 105, pp. 41~49.
- Mastrangelo, C. H., Zhang, X. and Tang, W.

- C., 1995, "Surface Micromachined Capacitive Differential Pressure sensor with Lithographically-Defined Silicon Diaphragm," in *Proceedings of the international Solid-State Sensors and Actuators Conference-TRANSDUCERS '95*, Vol. 1, 25-29, pp. 612~615.
- Timoshenko, S., 1940, "Theory of Plates and Shells," *McGraw-Hill Book Company*, New York.